Journal of Ceramic Processing Research. Vol. 26, No. 6, pp. 1043~1047 (2025)
(Received 12 August 2025, Received in revised form 29 October 2025, Accepted 21 November 2025)
https://doi.org/10.36410/jcpr.2025.26.6.1043

J O U R N A L O F
Ceramic Processing Research

Tuning τ_f of $Li_4Mg_2SbO_6F$ microwave dielectric ceramics through Li_2SnO_3 addition

Duanyuan Yang[a], Luyi Wang[a], Li Quan[a], Miao Chen[a], Yaming Zhang[a], Weihong Liu[b], Cuijin Pei[a], Guoguang Yao[a,*], Yansheng Wang[c] and Wei Zhang[a,*]
[a]*School of Science, Xi'an University of Posts and Telecommunications, Xi'an 710121, China*
[b]*School of Electronic Energineering, Xi'an University of Posts and Telecommunications, Xi'an 710121, China*
[c]*Xi'an Chaofan Optoelectronic Equipment Co., LTD, Xi'an 710121, China*

Microwave ceramics with low dielectric constant (ε_r<15), high quality factor (Q×f>50,000 GHz) and near-zero temperature coefficient of resonance frequency ($|\tau_f|\leq$10 ppm/°C) are drawing tremendous attentions for basic study and 5G communication. To obtain above parameters, the (1-*x*)$Li_4Mg_2SbO_6F$–*x*Li_2SnO_3 (*x*=0.65-0.85) composite ceramics were fabricated through a solid state reaction route at 825-900 °C. X-ray diffraction analysis showed two phase coexistence of cubic structural $Li_4Mg_2SbO_6F$ and monoclinic structural Li_2SnO_3. The microwave dielectric properties (MDPs) of $Li_4Mg_2SbO_6F$-host counterpart is significantly improved with an amount of Li_2SnO_3 addition (*x*=0.75). For the *x*=0.75 composition, with increment of sintering temperature, its volume density and dielectric constant (ε_r) rose little by little, its quality factor (Q×f) rose first and then decreased, and its temperature coefficient of resonance frequency (τ_f) remained stable. Optimum MDPs with a ε_r of 12.9, Q×f of 60, 100 GHz and τ_f of -10.6 ppm/°C were achieved at *x*=0.75 composition sintered at 875 °C, this ceramics also exhibited good co-firing chemical compatibility with silver electrode.

Keywords: Diphase ceramics, $Li_4Mg_2SbO_6F$ oxyfluorides, Near-zero temperature coefficient.

Introduction

Recently, Li-containing oxyfluoride ceramics are drawing tremendous attentions owing to their fascinating low sintering temperature as well as eminent MDPs [1-4]. Within the Sb_2O_5-LiF–Li_2O–MgO system, a novel oxyfluoride namely, $Li_4Mg_2SbO_6F$, was reported. We found that the 750 °C-sintered $Li_4Mg_2SbO_6F$ oxyfluoride ceramics possess eminent MDPs at 11.3 GHz (ε_r=12.6, Q × f = 59, 000 GHz, τ_f = -37 ppm/°C) [5]. However, its poor τ_f value (-37 ppm/°C) of $Li_4Mg_2SbO_6F$ oxyfluoride ceramics impedes its use in LTCC applications in a large measure [6]. There are two mainstream methods to modulate the MDPs, especially for τ_f, that is selecting two compounds with converse τ_f to construct diphase ceramics and ion replacement to construct a solid solution [7-10]. The solid solution $LiIn_{1-x}Ga_xO_2$ (*x* = 0.1, $\tau_f \approx$ +10.1 ppm/°C) and (1-*x*)$Mg(Zr_{0.05}Ti_{0.95})O_3$–*x*$SrTiO_3$ diphase ceramics (*x* = 0.04, $\tau_f \sim$ +10.1 ppm/°C) are the most suitable samples among the situations aforementioned [11, 12].

In this paper, the Li_2SnO_3 with positive τ_f (26.9 ppm/°C) was introduced to tune the MDPs of $Li_4Mg_2SbO_6F$-basic ceramics [13, 14]. Thus, the (1-*x*)$Li_4Mg_2SbO_6F$–*x*Li_2SnO_3 (*x*=0.65-0.85) diphase ceramics were designed and fabricated via a solid state reaction at 825-900 °C. The influence of Li_2SnO_3 addition on the phase assemble, sinterability, microstructures along with MDPs of 0.25$Li_4Mg_2SbO_6F$–0.75Li_2SnO_3 sintered specimens was thoroughly investigated.

Experimental

Through a solid-state process the (1-*x*)$Li_4Mg_2SbO_6F$–*x*Li_2SnO_3 (*x*=0.65-0.85) (abbreviated as LMSOF-LSO) specimens were fabricated [15]. Based on stoichiometric $Li_4Mg_2SbO_6F$ and Li_2SnO_3, the initial materials of MgO, Li_2CO_3, LiF, Sb_2O_5, SnO_2 (all purity >98.0%) were separately weighed, then were individually mixed via planetary milling for 9 h with anhydrous alcohol as medium. The dried $Li_4Mg_2SbO_6F$ and Li_2SnO_3 slurries were individually presintered under 550 °C/5 h and 950 °C/5 h. Subsequently, the LMSOF-LSO mixture powders were re-milled for 9 h. By adding 6 wt% PVA binder, the above mixture powders were granulated, and compacted into green discs with diameter of 10 mm and thickness around 4.5 mm. Finally, these discs were fired under 825 °C–900 °C for 5 h in air atmosphere.

The phase identification, structural investigation along with surface morphology of the LMSOF-LSO samples were examined via X-ray diffraction (XRD, Japan)

*Corresponding author:
Tel : +86 29 88166089
Fax: +86 29 88166333
E-mail: yaoguoguang@xupt.edu.cn, zhangweio@xiyou.edu.cn

and scanning electron microscopy (SEM, Czech). The volume densities of fired specimens were trialed employing Archimedes' drainage approach [16]. With the help of resonant cavity method, the ε_r and Qxf values under microwave region about 10-11 GHz of the LMSOF-LSO ceramics were measured employing a vector network analyzer (Ceyer 3674D). The τ_f values were evaluated based on following expressions (1) [17].

$$\tau_f = \frac{f_{85} - f_{25}}{f_{25} \times (85 - 25)} \quad (1)$$

Results and Discussion

Table 1 summarizes the microwave dielectric properties of 875 °C-sintered LMSOF-LSO ceramics systems. As x rose from 0.65 to 0.85, the ε_r values first increased and then decreased, while the $|\tau_f|$ and Qxf values gradually decreased. The good comprehensive MDPs could be obtained for the composition of x=0.75. Therefore, the following research was focused on the x=0.75 composition ceramics.

Fig. 1 gives the XRD plots of 0.25LMSOF-0.75LSO ceramics under diverse temperature sintering. All samples exhibited a similar phase assemble. All diffraction peaks match well with MgO-like (PDF #77-2364) cubic structural phase of $Li_4Mg_2SbO_6F$ and monoclinic structural phase of Li_2SnO_3 (PDF #76-1149). The achieved outcomes indicated the formation of a $Li_4Mg_2SbO_6F$/Li_2SnO_3 diphase ceramics without noticeable secondary phases, which could attribute to their diverse crystal structure [18].

Table 1. Microwave dielectric properties of 875 °C-sintered (1-x)LMSOF-xLSO ceramics.

Composition	ε_r	Qxf (GHz)	τ_f (ppm/°C)
x=0.65	12.7	64,650	−18.5
x=0.75	12.9	60,100	−10.6
x=0.85	12.0	11,540	−2.3

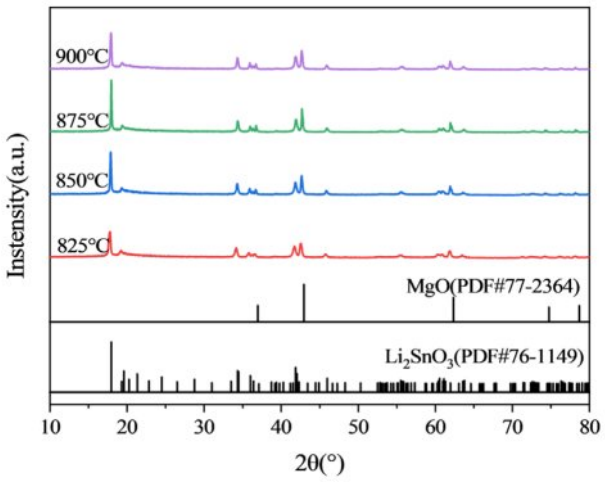

Fig. 1. The XRD plots of 0.25LMSOF-0.75LSO under different temperature sintering.

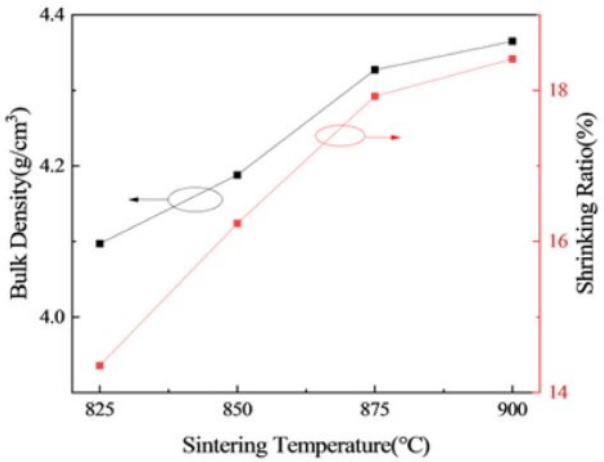

Fig. 2. The density and shrinkage of 0.25LMSOF-0.75LSO under different temperature sintering.

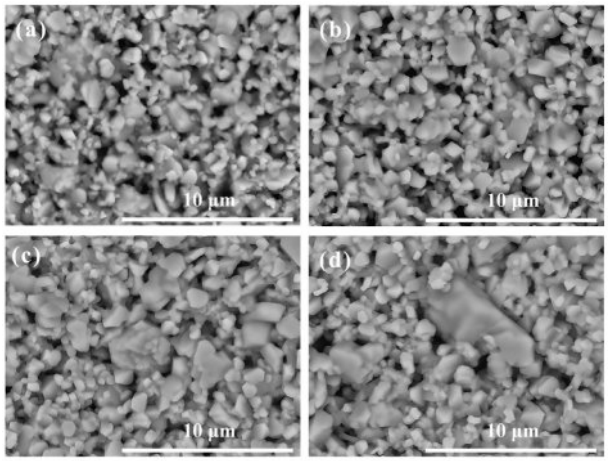

Fig. 3. The surface morphology of the 0.25LMSOF-0.75LSO samples under different temperature sintering: (a) 825 °C, (b) 850 °C, (c) 875 °C, (d) 900 °C.

The density and shrinking ratio of 0.25LMSOF-0.75LSO under different temperature sintering are given in Fig. 2. The density and shrinking ratio showed a similar tendency, that is a whole enhancing tendency as the sintering temperature rose. This could attribute to that the gases from the pores within the ceramics flee with an increasement in firing temperature, the ceramics shrinks and thus results in its density increment [19, 20].

Fig. 3(a)-(e) display the typical SEM graphs of 0.25LMSOF-0.75LSO heated at 825-900 °C. All samples do not look very dense. When the samples were heated at 825 °C, numerous intergranular pores were observed, which tallied well with its poor density, as illustrated in Fig. 2 and Fig. 3(a). As the firing temperature rose, the amount of intergranular pores declined little by little, and a comparatively compact microstructure were

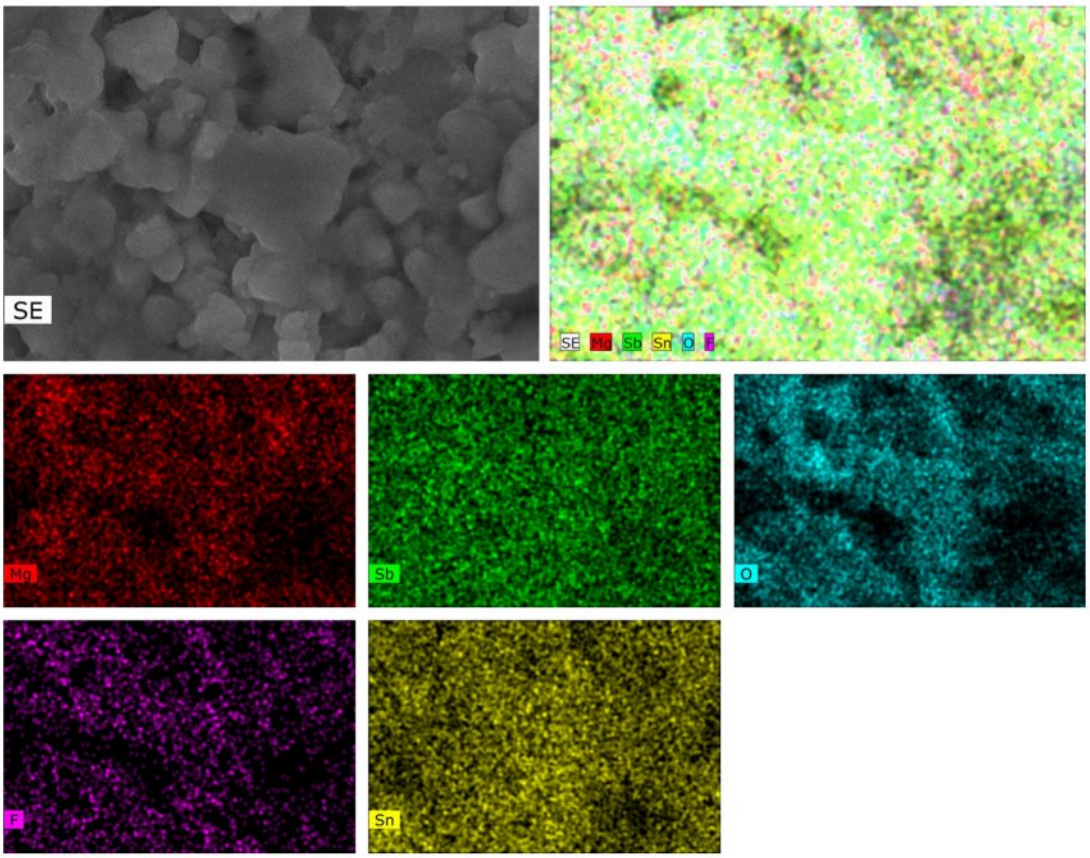

Fig. 4. Energy-dispersive spectroscopy elemental mapping results of 0.25LMSOF-0.75LSO ceramics sintered at 875 °C.

gained for 875 °C-heated ceramics. Further increment the heating temperature to 900 °C, an abnormal grain growth emerged, as seen in Fig. 3(d). Moreover, all samples owned two distinct-colored grains (light and black) and similar grain shape, which tallied well with the aforementioned XRD results. To identify the phase composition of distinct-colored grains, the energy dispersive spectrometer was carried out on the 0.25LMSOF-0.75LSO ceramics sintered at 875 °C, as shown in Fig. 4. The elemental mappings results reveal local enrichment of Mg, Sb, and F elements, whereas the Sn element is distributed throughout the entire region, which is slightly different from the XRD results.

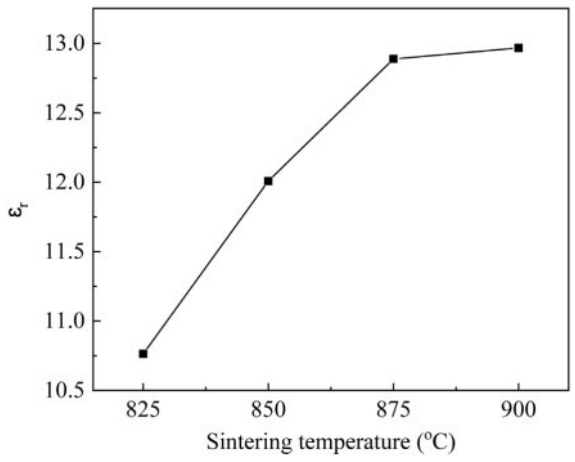

Fig. 5. The ε_r of the 0.25LMSOF-0.75LSO samples under different sintering temperature.

The dependence of ε_r over sintering temperature of the 0.25LMSOF-0.75LSO samples is exhibits in Fig. 5. The reliance of ε_r upon sintering temperature almost shows a similar inclination to that of densities (Fig. 2), since ε_r in microwave frequency is chiefly influenced by porosity for given composition [21]. The ε_r of present ceramics increased little by little from 10.7 to 13.0 upon enhancing sintering temperature, which is tightly connected with the reduce in porosity, considering the ε_r of pores is nearly equal to 1.

Fig. 6 exhibits the dependence of Q×f and τ_f of the 0.25LMSOF-0.75LSO samples on firing temperature. The change tendency of Q×f values over sintering temperature is not quite the same as that the variation in either density or ε_r values. It is notice that the change in Q×f value over sintering temperature is far more sophisticated compared to the one in either density or ε_r. The present ceramics displayed a stepwise increment in Q×f values with the wake of firing temperature, achieve a peak value of 60, 100 GHz at 875 °C, and slightly declined in the end with further increasing temperature. The increment in Q×f values is due to the increment in density (Fig. 2), whereas the reduced Q×f values at 900

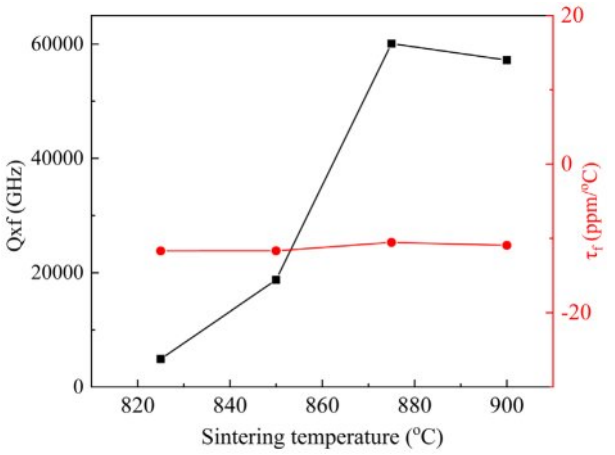

Fig. 6. The Q×f and τ_f of the 0.25LMSOF-0.75LSO samples under different sintering temperature.

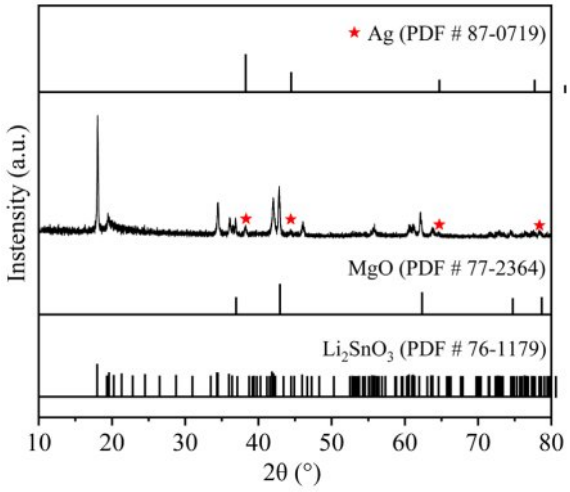

Fig. 7. The XRD pattern of the mixture of the 0.25LMSOF-0.75LSO and Ag fired at 875 °C.

°C is due to the observed an abnormal grain growth in Fig. 3(d). With regard to τ_f , as shown in Fig. 6, the τ_f values is irrelevant to sintering temperature and can remain relatively stable at approximately −10.6 ppm/°C. The τ_f value is well-known to be influenced by the composition, the additive and the second phase of the materials [22-24]. In current ceramics, the relatively stable τ_f can attribute to its unchanged phase assemble of $Li_4Mg_2SbO_6F$ and Li_2SnO_3 (seen in Fig. 1), where $Li_4Mg_2SbO_6F$ owns negative τ_f (-37 ppm/°C) and Li_2SnO_3 owns positive owns negative τ_f (26.9 ppm/°C) [5, 13].

To ensure the LTCC applicability of the present ceramic, good chemical compatibility with Ag electrode during sintering is necessary. Thus, the XRD was conducted to assess the compatibility of between 0.25LMSOF-0.75LSO composition and Ag electrode fired at 875 °C, and corresponding result is shown in Fig. 7. As the XRD pattern does not show the formation of any secondary phase except for $Li_4Mg_2SbO_6F$, Li_2SnO_3 and Ag phases, suggesting well co-firing chemical compatibility of the 0.25LMSOF-0.75LSO ceramics with Ag electrode.

Table 2 showcases the microwave dielectric properties of Li-based oxyfluorides ceramics. Compared to other ceramics except $Li_2Mg_2GaTi_2O_8F$, our 0.25LMSOF-0.75LSO ceramics has excellent comprehensive properties, including low ε_r, low sintering temperature dielectric, near-zero τ_f and high or comparable Q×f.

Conclusions

In this work, (1-*x*)$Li_4Mg_2SbO_6F$–*x*Li_2SnO_3 (*x*=0.65-0.85) composite ceramics were fabricated through a solid state reaction route at 825-900 °C. The diphase ceramics of cubic structural $Li_4Mg_2SbO_6F$ and monoclinic structural Li_2SnO_3 could coexist harmoniously as confirmed by XRD analysis. The introduction of Li_2SnO_3 can not only significantly ameliorate the τ_f, but also improve the Q×f and ε_r of $Li_4Mg_2SbO_6F$-host counterpart. For the *x*=0.75 composition, its ε_r is chiefly influenced by density, its Q×f is chiefly influenced by density and overinflated grain coarsening, and its τ_f is chiefly influenced phase assemble. The excellent MDPs with a ε_r of 12.9, Q×f of 60,100 GHz and τ_f of -10.6 ppm/°C along with its well co-firing chemical compatibility with Ag electrode for *x*=0.75 composition ceramics, make it a prospective material for LTCC applications.

Acknowledgements

This work was funded by grants from National Natural Science Foundation of China (No. 52272122, No. 52002317), Service Local Special Plan Project of Shaanxi Province Education Department (No. 24JC082), Xi'an Sciences Plan Project (No. 24GXFW0084, No. 25GXKJRC00053), Undergraduate Innovation and Entrepreneurship Training Program in Shaanxi Province

Table 2. Comparison of microwave dielectric properties of Li-based oxyfluorides ceramics.

Composition	Ts(°C)	ε_r	$Q\times f$ (GHz)	τ_f (ppm/°C)	Reference
$Li_2Y_9(SiO_4)_6O_2F$	1275	14.28	16,760	3.14	1
$Li_{0.5}NaY_9(SiO_4)_6O_2F_{0.5}$	1525	12.34	35,597	-28.2	2
$Li_2Mg_2GaTi_2O_8F$	1050	14.58	76,689	-52.0	3
$Li_{4.75}Ti_2Mg_7O_{13}F_{0.75}$	925	14.99	137,180	-36.5	25
$0.75Li_4Mg_2SbO_6F$-$.25Li_2SnO_3$	875	12.90	60,100	-10.6	this work

(No. S202511664075).

References

1. D.Y. Liang, T.T. Liao, F. Dong, B. Tang, and F. Si, J. Electron. Mater. 53 (2024) 3223-3230.
2. Z.X. Fang, H.F. Peng, D.Y. Liang, Y.X. Li, B. Tang, and M. Zhang. Ceram. Int. 50 (2024) 43513-43521.
3. Z.G. Hou, Y.X. Li, F. Wang, D.Y. Liang, B. Tang, and W. Liu, Ceram. Int. 50 (2024) 46542-46547.
4. P.S. Wu, C.J. Pei, M. Chen, X. Gao, W.H. Liu, G.G. Yao, and J. Liu, J. Ceram. Process. Res. 24[6] (2023) 977-982.
5. C.J. Pei, H.K. Liu, M. Chen, F. Shang, W.H. Liu, and G.G. Yao, Ceram. Int. 50 (2024) 51718-51723.
6. C.L. Huang,Y.Q. Guan, M. Huang, F.L. Wang, W. Li, H.J. Mao, Z.F. Liu, W.J. Zhang, and X.Y. Chen, Ceram. Int. 51 (2025) 13507-13513.
7. F.L. Liu, J. Li, Y.H. Sun, Y. Tang, and L. Fang, Ceram. Int. 51 (2025) 7370-7376.
8. G.G. Yao, J.J. Tan, J.X. Yan, M.Q. Liu, C.J. Pei, and Y.M. Jia, Ceram. Int. 47 (2021) 27406-27410.
9. A.R.H. Alzakree, C.H. Wan, and M. Shehbaz, J. Am. Ceram. Soc. 108 (2025) e20504.
10. C.H. Shen, C.H. Hu, J.Y. Chen, W.H. Chen, C.W. Tung, Y.H. Yang, and T.Y. Yang, J. Ceram. Process. Res. 25[5] (2024) 790-797.
11. J.W. Chen, J.J. An, J.Q. Chen, and L. Fang, J. Mater Sci: Mater. Electron. 36 (2025) 938.
12. T. Ahmed, J.H. Lee, M.Y. Kim, S.A. Khan, H.T. Kim, G.Y. Lee, D.H. Yeo, and S. Lee, J. Eur. Ceram. Soc. 44 (2024) 6987-6994.
13. X. Chu, L. Gan, J.Jiang, J.Z. Wang, and T.J. Zhang, Mater. Today Commun. 37 (2023) 107145.
14. L.X. Pang, and D. Zhou, J. Am. Ceram. Soc. 93 (2010) 3614-3617.
15. P.C. Chen, C.L. Pan, K.C. Lin, and C.H. Shen, J. Ceram. Process. Res. 25[2] (2024) 278-284.
16. J.H. Liu, Z. Lu, Y.G. Jung, Y. Li, Y.W. Zhou, H. Chen, J.H. Son, H.K. Choi, and J.S. Lee, J. Ceram. Process. Res. 26[3] (2025) 386-396.
17. H. Liu, L. Cao, and K. X. Song, J. Eur. Ceram. Soc. 45 (2025) 116957.
18. G.G. Yao, Z.Y. Ren, and P. Liu, J. Electroceram. 40 (2018) 144-149.
19. Y.J. Liu, G.Q. He, and H.F. Zhou, Ceram. Int. 50 (2024) 36440-36447.
20. Z.H. Huang, D.P. Wang, X.Y. Wu, W. Li, and W.T. Wang, J. Ceram. Process. Res. 26[1] (2025) 37-42.
21. X.H. Zhang, X.H. Zhang, S. Ma, X.Y. Qi, and Z.X. Yue, Ceram. Int. 50 (2024) 15831-15839.
22. X.S. Lv, L.X. Li, H. Sun, S. Li, and S. Zhang, Ceram. Int. 41 (2015) 15287-15291.
23. H.J. Wang and J.J. Bian, J. Eur. Ceram. Soc. 44 (2024) 2144-2149.
24. R.Z. Zuo, J. Zhang, J. Song, and Y.D. Xu, J. Am. Ceram. Soc. 101 (2018) 569-576.
25. R. Li, X.B. Zhou, S.M. Zhai, S.F. Hou, P. Shi, and P. Liu, Ceram. Int. 51 (2025) 8824-8831.